Preclinical Development

Molecular Cancer Therapeutics

Targeting the Insulin Growth Factor and the Vascular Endothelial Growth Factor Pathways in Ovarian Cancer

Minghai Shao[1], Stacy Hollar[1], Daphne Chambliss[1], Jordan Schmitt[1], Robert Emerson[2], Bhadrani Chelladurai[1], Susan Perkins[1,6], Mircea Ivan[1,3,6], and Daniela Matei[1,4,5,6,7]

Abstract

Antiangiogenic therapy is emerging as a highly promising strategy for the treatment of ovarian cancer, but the clinical benefits are usually transitory. The purpose of this study was to identify and target alternative angiogenic pathways that are upregulated in ovarian xenografts during treatment with bevacizumab. For this, angiogenesis-focused gene expression arrays were used to measure gene expression levels in SKOV3 and A2780 serous ovarian xenografts treated with bevacizumab or control. Reverse transcription-PCR was used for results validation. The insulin growth factor 1 (IGF-1) was found upregulated in tumor and stromal cells in the two ovarian xenograft models treated with bevacizumab. Cixutumumab was used to block IGF-1 signaling *in vivo*. Dual anti-VEGF and IGF blockade with bevacizumab and cixutumumab resulted in increased inhibition of tumor growth. Immunohistochemistry measured multivessel density, Akt activation, and cell proliferation, whereas terminal deoxynucleotidyl transferase–mediated dUTP nick end labeling (TUNEL) assay measured apoptosis in ovarian cancer xenografts. Bevacizumab and cixutumumab combination increased tumor cell apoptosis *in vivo* compared with therapy targeting either individual pathway. The combination blocked angiogenesis and cell proliferation but not more significantly than each antibody alone. In summary, IGF-1 activation represents an important mechanism of adaptive escape during anti-VEGF therapy in ovarian cancer. This study provides the rationale for designing bevacizumab-based combination regimens to enhance antitumor activity. *Mol Cancer Ther; 11(7); 1576–86. ©2012 AACR.*

Introduction

Ovarian cancer arises from the epithelial layer covering the surface of ovaries and metastasizes intraperitoneally (i.p.). Tumor growth and metastasis rely heavily on efficient development of new blood vessels (1). The peritoneal environment is rich in secreted factors, including VEGF (2), lysophophatidic acid (3), platelet-derived growth factor (PDGF; ref. 4), TGF-β, and others, which stimulate angiogenesis and growth of ovarian tumors. Angiogenic signatures correlate tightly with survival of patients with ovarian cancer (5), underscoring the significance of angiogenesis to ovarian tumor progression. Of these factors, VEGF plays a significant role. Immunostaining detects VEGF expression in most ovarian tumors and omental metastases, and VEGF is measurable in ovarian cancer patients' ascites and serum (6). VEGF and VEGFR-2 expression levels in ovarian tumors are independent poor prognostic factors (7–9) and correlate with surgical stage (10). VEGF is secreted in malignant ascites at concentrations 50 to 200 times higher than in nonmalignant fluid (11) and serum VEGF concentrations correlate with prognosis (12).

Antiangiogenic therapy (AAT) and particularly anti-VEGF strategies have direct inhibitory effects on blood vessels and may also block the proliferation of ovarian cancer cells (13). Anti-VEGF agents inhibit angiogenesis, destroy existent vessels, and facilitate normalization of abnormally tortuous and fenestrated vessels (14, 15). The effects on blood vessels lead to increasing hypoxia, nutrient deprivation, and other dynamic changes in the tumor microenvironment causing arrest of proliferation and/or apoptosis of cancer cells (16).

Recent phase II studies have indicated that AAT is highly effective in ovarian cancer (17–20). On the basis of those results, bevacizumab, a humanized monoclonal antibody to VEGF was investigated in the upfront treatment of advanced stage ovarian cancer along with chemotherapy (GOG protocol 218 and ICON 7; refs. 21, 22). The recent results of these studies showed improvement in progression-free survival for women treated with bevacizumab in combination with standard chemotherapy, bringing the agent to the forefront of ovarian cancer adjuvant therapy. However, although patients with ovarian cancer derive initial clinical benefit from bevacizumab,

Authors' Affiliations: Departments of [1]Medicine, [2]Pathology, [3]Microbiology and Immunology, [4]Biochemistry and Molecular Biology, and [5]Obstetrics and Gynecology, [6]Melvin and Bren Simon Cancer Center, and [7]VA Roudebush Hospital, Indiana University School of Medicine, Indianapolis, Indiana

Corresponding Author: Daniela Matei, Indiana University Simon Cancer Center, 535 Barnhill Drive, RT 473, Indianapolis, IN 46202. Phone: 317-278-8844; Fax: 317-278-0074; E-mail: dmatei@iupui.edu

doi: 10.1158/1535-7163.MCT-11-0961

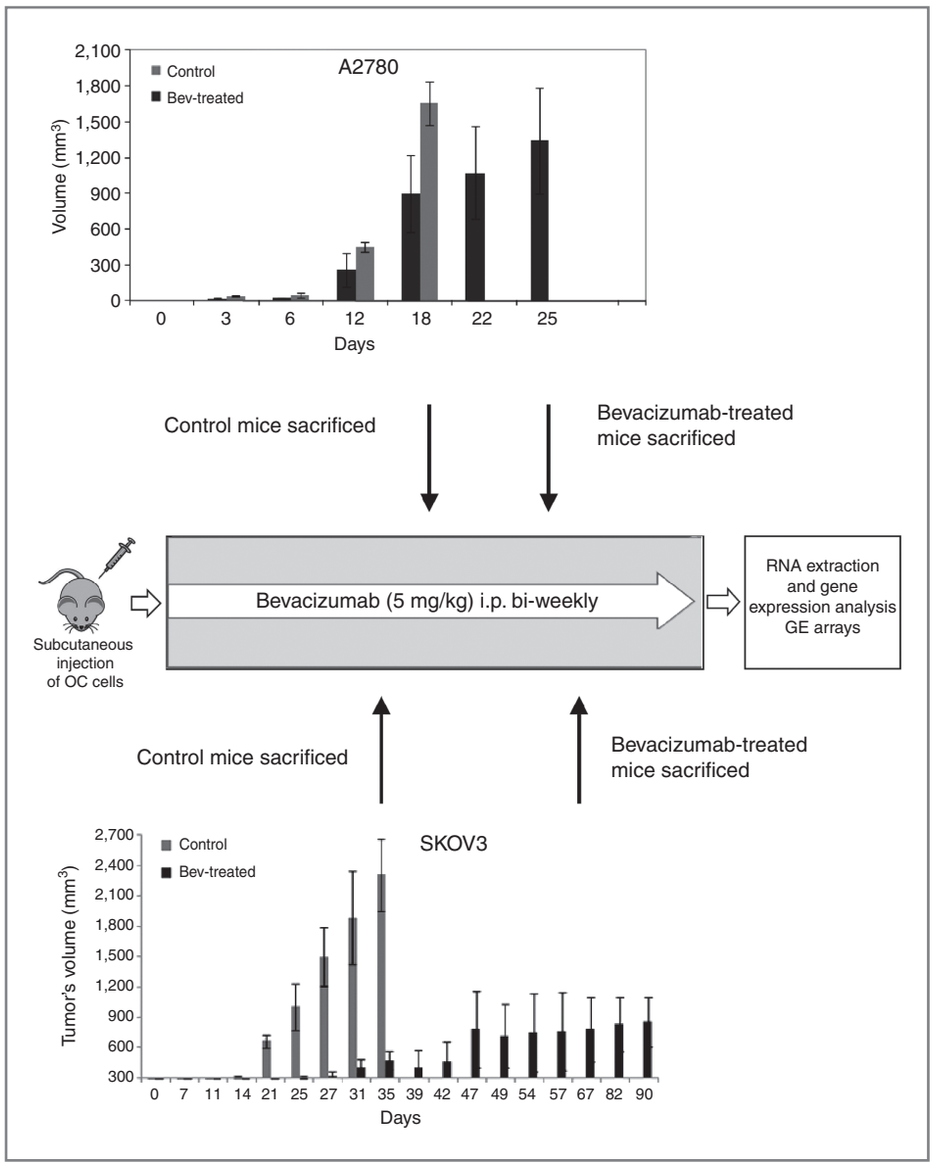

Figure 1. Flow chart illustrates design of experiments using bevacizumab (Bev) in ovarian xenografts and tumor response over time. Two ovarian cancer cell lines SKOV3 and A2780 were used. GE, gene expression.

this is usually transitory and has not translated into improved long-term survival (21, 22).

It has been speculated that under the pressure of AAT, adaptive escape and survival pathways emerge, facilitating alternative mechanisms of growth or metastasis. For instance, in one study using glioblastoma and pancreatic islet tumors, anti-VEGF therapy elicited activation of the Met pathway leading to increased tumor invasiveness (23–25). In another study using melanoma and sarcoma models, treatment with anti-VEGF antibody increased recruitment of myeloid cells ($Gr1^+$) to the necrotic areas of tumors, altering the proinflammatory milieu (26, 27) that led to increased propensity to metastasis. We hypothesized that such adaptive mechanisms are activated in ovarian tumors treated with bevacizumab and set out to explore alterations of angiogenesis-related gene expression levels in ovarian cancer xenografts treated with bevacizumab by using pathway-focused gene expression arrays.

Here, we report that the insulin growth factor-1 (IGF-1) is upregulated during treatment with bevacizumab of ovarian xenografts and show that dual anti-VEGF and IGF blockade results in enhanced tumor growth inhibition compared with therapy targeting a single pathway. These results point to IGF-1 upregulation as representing an important mechanism of adaptive escape during anti-VEGF therapy in ovarian cancer and provide the rationale for designing bevacizumab-based combination regimens to increase antitumor activity.

Materials and Methods

Ovarian cancer cell lines and materials

SKOV3 ovarian cancer cells were from the American Type Culture Collection. A2780 cells were a gift from

Table 1. Genes induced by bevacizumab treatment in ovarian xenografts

Gene symbol	Gene name	Fold difference	*P*
A2780			
ID-1	Inhibitor of DNA binding 1	2.50	0.005
TNFAIP2	TNF-α–induced protein 2	6.64	0.039
IGF-1	Insulin growth factor 1	3.58	0.027
HPSE	Heparanase	2.38	0.025
THBS-1	Thrombospondin 1	1.95	0.014
THBS-2	Thrombospondin 2	1.73	0.044
TIMP-1	TIMP metallopeptidase inhibitor 1	1.82	0.041
SKOV3			
ANGPTL3	Angiopoietin-like 3	11.62	0.0243
COL4A3	Collagen, type IV, α 3 (Goodpasture antigen)	6.87	0.04
IGF-1	Insulin growth factor 1	7.07	0.045
IL-1β	Interleukin-1β	5.24	0.044
S1PR-1	Sphingosine-1-phosphate receptor 1	1.95	0.045

Dr. J. Turchi of Indiana University (Indianapolis, IN) and human umbilical vein endothelial cell (HUVEC) cells were from Cell Applications. The cells were not authenticated. SKOV3 cells were cultured in growth media containing 1:1 MCDB 105 (Sigma) and M199 (CellGro), A2780 cells were grown in Dulbecco's Modified Eagle's Medium (Sigma), and HUVEC cells were cultured in endothelial growth media supplemented with growth factors, as per provider's instructions (Cell Applications). Cancer cell media was supplemented with 10% heat-inactivated FBS (CellGro) and 1% antibiotics (100 units/mL penicillin and 100 μg/mL streptomycin) and cells were grown at 37°C in a humidified 5% CO_2 atmosphere. Cixutumumab was provided by Dr. Ruslan Novosyadlyy of Imclone and bevacizumab was purchased from Indiana University Pharmacy. *In vitro* treatment with cixutumumab and bevacizumab used 20 and 75 μg/mL, respectively, for 3 days.

In vivo anti-VEGF and IGF therapy

Seven to 8-week-old female nude mice (*nu/nu* BALB/c) were purchased from Harlan. Animal procedures were approved by the Indiana University School of Medicine Animal Care and Use Committee and were in accordance with federal regulations. After acclimatization, A2780 cells or SKOV3 cells (5×10^6 cells/mouse) were injected subcutaneously in the right flank. Tumors were measured weekly with calipers, and tumor volume in mm^3 was calculated according to the formula: volume = $width^2 \times length/2$. Treatments were started when tumors became measurable, usually within 1 week of s.c. tumor implantation. To study tumor response to bevacizumab, the agent was administered i.p. at a dose of 5 mg/kg twice a week. Control mice were treated with 0.9% sodium chloride. Treatment was continued until tumors exceeded 2 cm^3 or animals showed signs of distress, at which point mice were sacrificed and tumors were harvested, measured, and snap frozen. When possible, tumors from each group were minced in the presence of hyaluronidase at a concentration of 1 mg/mL and cultured. The xenograft-derived cultures were characterized by proliferation (MTT) and clonogenic assays.

To measure response to bevacizumab and cixutumumab, mice were treated with bevacizumab (5 mg/kg, i.p., twice a week); cixutumumab (60 mg/kg, i.p., twice a week); bevacizumab and cixutumumab (5 mg/kg, i.p., and 60 mg/kg i.p., respectively, twice a week), or v/v saline control i.p. Each experimental group consisted of 5 to 6 animals. Both cell lines (SKOV3 and A2780) were tested. Treatment continued for up to 3 weeks (A2780 cells) and 6 weeks (SKOV3 cells), at which point mice were euthanized, tumors harvested and paraffin embedded for future studies.

Angiogenesis PCR array

RNA was extracted from tumors harvested and snap frozen from control and bevacizumab-treated animals ($n = 3$ per group and per cell line), by using the RNA STAT-60 reagent (Tel-Test, Inc.). RNA was reverse-transcribed using the RT2 First Strand Kit (C-03; SA Biosciences), according to the manufacturer's instructions. Genomic DNA contamination was eliminated by DNAse treatment by using RNEasy Micro Kit (Qiagen GmbH). Human Angiogenesis RT^2 Profiler PCR Array and RT^2 Real-Timer SyBR Green/ROX PCR Mix were purchased from SA Bioscience Corporation. PCR was carried out on ABI Prism 7900 Sequence Detector (Applied Biosystems). For data analysis, the $\Delta\Delta C_t$ method was used; for each gene, fold-changes being calculated as difference in gene expression between control and bevacizumab-treated groups. A positive value indicated gene upregulation and a negative value indicated gene downregulation.

Reverse transcriptase PCR

RNA extracted from xenografts by using the RNA STAT-60 reagent (Tel-Test, Inc.) was reverse-transcribed

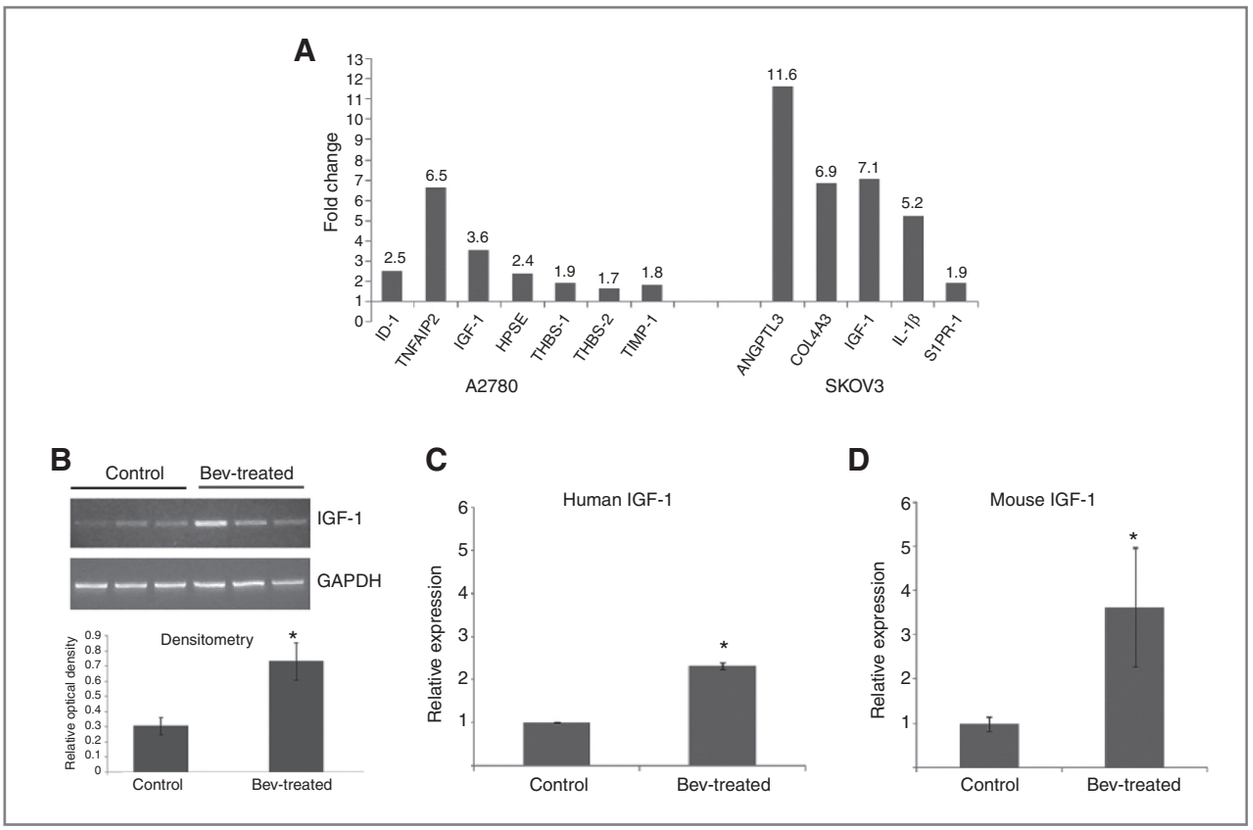

Figure 2. IGF-1 expression upregulation in ovarian xenografts treated with bevacizumab. A, fold increase in gene expression levels induced by bevacizumab treatment in ovarian xenografts, as measured by gene expression arrays. B, semiquantitative RT-PCR for human IGF-1 in control ($n = 3$) and bevacizumab ($n = 3$)-treated A2780 xenografts (top) and densitometry analysis (bottom). C, qRT-PCR for human IGF-1 in control ($n = 3$) and bevacizumab ($n = 3$)-treated A2780 xenografts (left). D, qRT-PCR for murine IGF-1 in control ($n = 3$) and bevacizumab ($n = 3$)-treated A2780 xenografts (right).

using the iScript cDNA synthesis kit (Bio-Rad). The PCR reactions used Taq polymerase (Promega) and the following primers: IGF-1 (forward): 5′-CCTGCGCAATGGAATAAAGT-3′, (reverse): 5′-TCAAATGTACTTCCTTCTGGGTC-3′; GAPDH (forward): 5′-GATTCCACCCATGGCAAATTCC-3′; (reverse): 5′-CACGTTGGCAGTGGGGAC-3′. For real-time PCR, we used the FastStart TaqMan Probe Master (Rox, Roche) on an ABI Prism 7900 platform (Applied Biosystems) according to the manufacturer's procedures. The primers and probes used are enclosed in Supplementary Table S1. At the end of the PCR reaction, a melting curve was generated and the cycle threshold (C_t) was recorded for the reference gene and for glyceraldehyde-3-phosphate dehydrogenase (GAPDH). Relative expression of gene of interest was calculated as ΔC_t, measured by subtracting the C_t of the reference gene from that of the control. Results are presented as mean ± SD of replicates. Each measurement was carried out in duplicate and repeated in independent conditions.

Western blotting

Tumors were minced on ice and resuspended in radioimmunoprecipitation assay buffer containing protease inhibitors leupeptin (1 μg/mL), aprotinin (1 μg/mL), phenylmethylsulfonyl fluoride (PMSF; 400 μmol/L), and sodium orthovanadate (Na_3VO_4; 1 mmol/L). Tumor or cell lysates were sonicated briefly and subjected to centrifugation at 14,000 rpm for 15 minutes at 4°C to sediment particulate material. Equal amounts of protein (50 μg) were separated by SDS–PAGE and electroblotted onto polyvinylidene difluoride membranes (Millipore). After blocking, membranes were probed with primary antibody overnight at 4°C with gentle rocking. Antibodies used are GAPDH (1:5,000 dilution; Biodesign International), total IGF-1 receptor β, phospho-IGF-1 receptor β ($Tyr^{1150/1151}$), phospho-IRS-1 (Ser^{307}), VEGFR-2 (Cell Signaling), and Stat-5B (1:1,000; Santa Cruz; SC-1656). After incubation with specific horseradish peroxidase–conjugated secondary antibody, antigen–antibody complexes were visualized using the enhanced chemiluminescence detection system (Amersham Biosciences). Images were captured by a luminescent image analyzer with a CCD camera (LAS 3000, Fujifilm).

Immunohistochemistry

Immunohistochemistry evaluated multivessel density (MVD) by staining for CD31, cell proliferation by staining

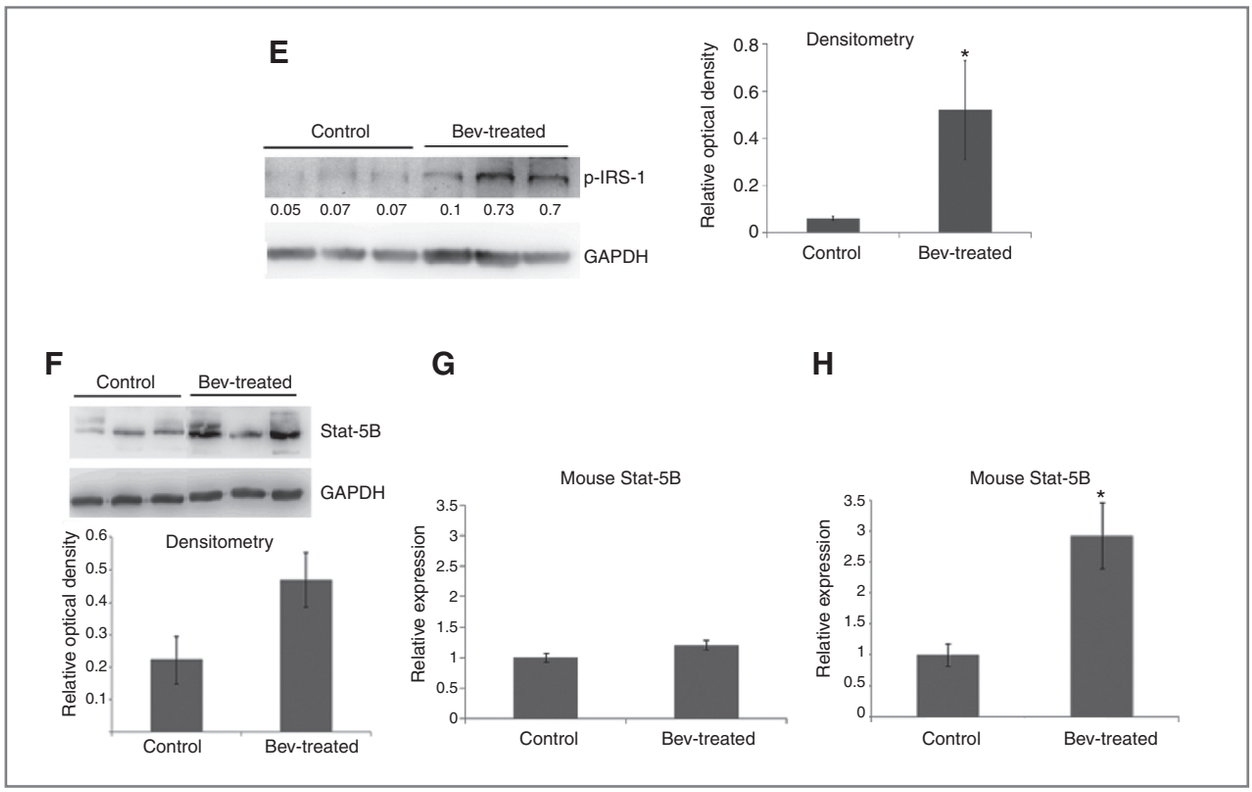

Figure 2. (*Continued*) E, phosphorylation of IRS-1 in SKOV3 xenografts treated with vehicle ($n = 3$) or bevacizumab ($n = 3$) was detected by Western blotting of homogenized tumor lysates (left). Densitometry analysis was conducted with Gel-Pro Analyzer 3.1 software (right). F, Western blotting for Stat-5b in control ($n = 3$) and bevacizumab ($n = 3$)-treated SKOV3 xenografts SKOV3 xenografts (top). Densitometry analysis was conducted with Gel-Pro Analyzer 3.1 software (bottom). G and H, qRT-PCR for human Stat-5b (G) and qRT-PCR for murine Stat-5b (H) in control ($n = 3$) and bevacizumab ($n = 3$)-treated A2780 xenografts. For human genes (IGF-1, STAT-5b) qRT-PCR, human GAPDH was used as endogenous control. For murine genes (IGF-1, STAT-5b), murine β-actin was used as endogenous control. Results are means ± SE of 3 mice per group; *, $P < 0.05$, significantly different from control.

for Ki67, and measured phospho-Ser^{473}-Akt on paraffin-embedded sections. Antibodies were from Cell Signaling (phospho-Akt, 1:100 dilution), Dako (Ki67, clone M7248, 1:100 dilution), and from Abcam (CD31, 1:250 dilution). After incubation with primary antibodies overnight at 4°C, detection was obtained with the avidin-biotin peroxidase technique using the DAKO Detection Kit (DAKO-Cytomation). For phospho-Akt, scoring used a 0–3+ scale for intensity and recording of the percentage of cells staining. An H score was calculated as the product between intensity and percentage of cells staining and compared between groups. For Ki67, the numbers of positive cells were counted per 5 high-power fields (HPF) per specimen and average values were compared between groups. MVD was assessed by counting the number of vessels lined by CD31-positive endothelial cells in 5 areas that appeared to have the highest vessel density per specimen. Numbers of vessels were averaged and compared between groups. Cell apoptosis was analyzed on frozen 5-μm thick tumor sections with *In Situ* Cell Death (Apoptosis) Detection allowing terminal deoxynucleotidyl transferase–mediated dUTP nick end labeling (TUNEL) labeling (Roche Applied Science), according to the manufacturer's instructions. Numbers of cells staining under UV excitation in 5 HPF per specimen were averaged for comparison between groups.

Statistical analysis

Statistical analyses were conducted using SAS version 9.3. Shapiro–Wilk and Levene tests were used to test normality and equal variance of the data, respectively. When normality and equal variance assumptions held, groups were compared using *t* tests or one-way ANOVA with significant overall tests followed by pairwise tests adjusted for multiple comparisons using the Student Newman–Keuls approach; otherwise Kruskal–Wallis tests were done with significant overall tests followed by pairwise exact Wilcoxon rank sum tests adjusted for multiple comparisons using the Hochberg–Bonferroni Step-Up approach. A *P* value of less than 0.05 was deemed significant. When an overall test was not significant, post hoc tests (*t* tests or exact Wilcoxon rank sum tests) were done to compare selected group combinations.

Results

IGF-1 is induced by treatment with bevacizumab in ovarian xenografts

Quantitative pathway-focused gene expression analysis was carried out in xenografts derived from 2 serous ovarian cancer cell lines (SKOV3 and A2780) after treatment with bevacizumab or control by using angiogenesis gene expression superarrays (Fig. 1). These arrays permit quantification of 92 angiogenesis-related genes and 6 housekeeping genes through quantitative RT-PCR methodology. Xenografts derived from A2780 cells had a doubling time of 4 days (control) versus 8 days (bevacizumab); whereas xenografts derived from SKOV3 cells had a doubling time of 7 days (control) versus 28 days (bevacizumab). Six genes were significantly upregulated in A2780 xenografts treated with bevacizumab compared with control, at a $P < 0.05$ level of significance: *ID-1*, *TNFα-induced protein 2*, *IGF-1*, *heparinase*, *thrombospondin-1* and *2*, and *tissue inhibitor of metalloproteinase (TIMP)-1* (Table 1, Fig. 2A). Five genes were upregulated in SKOV3 xenografts treated with bevacizumab compared with control: *angiopoietin-like 3*, *collagen type 4α3*, *IGF-1*, *interleukin-1β (IL-1β)*, and *sphingosine 1 phosphate receptor* ($P < 0.05$, Table 1, Fig. 2A). Cells derived from SKOV3 xenografts treated with bevacizumab had increased proliferation and clonogenic potential *in vitro* as compared with ovarian cancer cells derived from xenografts treated with vehicle (Supplementary Fig. S1A and S1B), suggesting that exposure to bevacizumab engages escape mechanisms that confer survival and proliferative advantage.

As IGF-1 was the only gene upregulated by bevacizumab in both xenograft models, and represents an important survival factor under stress conditions (28), we focused first on its validation and targeting. Semiquantitative and quantitative RT-PCR showed increased IGF-1 mRNA expression levels in A2780-derived xenografts treated with bevacizumab compared with control (Fig. 2B and C). Interestingly, both human (tumor-derived) and mouse (host-derived) IGF-1 levels were increased in bevacizumab-treated xenografts compared with controls (Fig. 2C and D) suggesting that both tumor and stromal cells secrete IGF-1 in the environment exposed to bevacizumab. Furthermore, phosphorylation of the insulin receptor substrate 1 (IRS-1), the adaptor protein that conveys signals from the activated IGF receptor to downstream pathways, was increased in bevacizumab-treated xenografts compared with controls (Fig. 2E). Collectively, these data support that the IGF-1 pathway is activated during anti-VEGF treatment of ovarian cancer xenografts.

It is known that IGF-1 is induced by cytokines and other growth factors and is transcriptionally regulated by STAT-5b (29, 30). We therefore measured protein and mRNA levels of STAT-5b in tumors treated with bevacizumab or control by Western blotting and by qRT-PCR. STAT-5b protein expression level was increased in SKOV3 xenografts during bevacizumab treatment (Fig. 2F), suggesting that this pathway is activated *in vivo*, perhaps contributing to IGF-1 induction. Tumor (human) STAT-5b was only modestly induced by bevacizumab treatment, whereas stromal (host) STAT-5b expression level was significantly increased in A2780 xenografts treated with bevacizumab versus control (Fig. 2G and H).

Anti-IGF and -VEGF therapy has antitumor effect *in vivo*

Based on the observation that IGF-1 is upregulated in xenografts exposed to bevacizumab, we hypothesized that combined therapy targeting the VEGF and IGF-1 pathways will exert potent antitumor effect. We tested this by using cixutumumab (IMC-A12; ImClone Systems), a fully human immunoglobulin G1 monoclonal antibody that inhibits IGF signaling (31, 32) in combination with bevacizumab. Cixutumumab prevents ligand binding to IGF-1 receptor and promotes receptor internalization and degradation. First, the effects of cixutumumab, bevacizumab, and the combination of the 2 antibodies were tested *in vitro* in endothelial (HUVEC) and tumor (SKOV3) cells. Treatment with cixutumumab or with cixutumumab and bevacizumab combination induced IGF-1 receptor expression level downregulation in HUVEC and SKOV3 cells, consistent with this antibody's known mechanism of action (Fig. 3A and B). As anticipated, treatment with bevacizumab did not affect IGF-1 receptor expression level. Interestingly, in HUVEC cells, bevacizumab and cixutumumab single agents also induced downregulation of VEGF receptor 2, the main receptor involved in VEGF signaling. The combination of cixutumumab and bevacizumab significantly downregulated VEGFR2 expression in HUVEC cells, as compared with each agent alone (Fig. 3A). These data suggest that cixutumumab has a direct effect on VEGFR 2 expression levels and that this effect is synergistic with bevacizumab's effects.

Next, the activity of cixutumumab, of bevacizumab, and of the combination of 2 antibodies was tested *in vivo* in A2780 and SKOV3 xenografts. As a single agent, cixutumumab modestly inhibited the growth of A2780 and SKOV3 subcutaneous xenografts whereas the combination of cixutumumab and bevacizumab exerted numerically superior effects as compared with each agent alone in both tumor models (Fig. 3C and D, $P < 0.05$ for overall tests).

Effects on tumor angiogenesis were measured by assessing MVD in SKOV3- and A2780-derived xenografts. Numerically, both single agents cixutumumab and bevacizumab decreased MVD in ovarian xenografts and the combination regimen further reduced MVD compared with each agent alone; however, the overall test was not statistically significant (Fig. 4A and B, $P = 0.05$ and Supplementary Fig. S2A and S2B). Apoptosis was measured by TUNEL staining in xenografts treated with control, cixutumumab, bevacizumab, and the 2 antibody combination (Fig. 4C and D, $P < 0.05$ for the overall test). Increased apoptosis was induced by the combination bevacizumab and cixutumumab, but not by single agent anti-VEGF or anti-IGF-1R antibody.

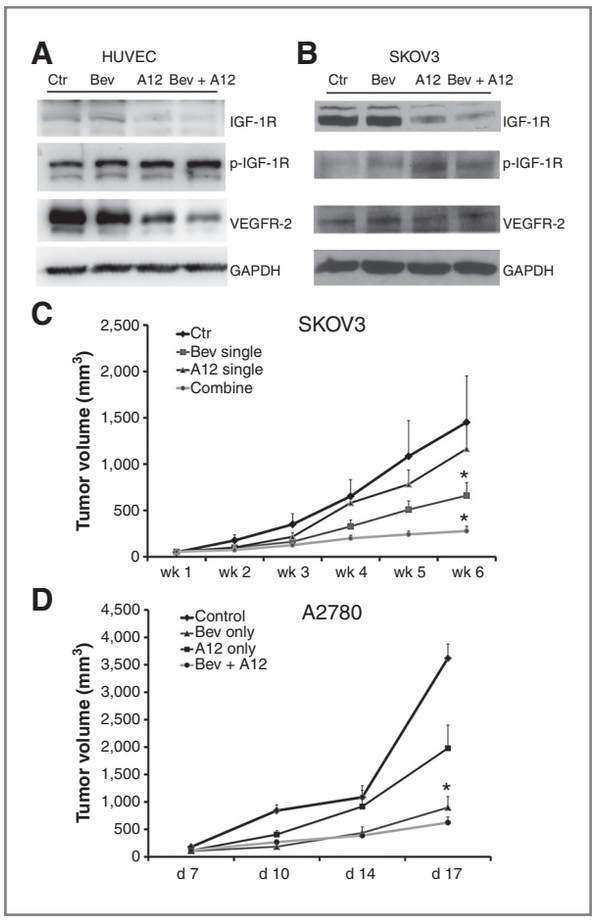

Figure 3. Effects of bevacizumab, cixutumumab, and combination bevacizumab and cixutumumab *in vitro* and *in vivo*. A, Western blotting for IGF-1 receptor β, VEGFR-2, and phospho-IGF-1 receptor β in HUVEC cells treated with cixutumumab (20 μg/mL), bevacizumab (75 μg/mL), and the combination of cixutumumab and bevacizumab. GAPDH was used as control. B, Western blotting for IGF-1 receptor β, VEGFR-2, and p-IGF-1 receptor β in SKOV3 cells treated with cixutumumab (20 μg/mL), bevacizumab (75 μg/mL), and the combination. GAPDH was used as control. C, growth curve for SKOV3 xenografts. Results are means ± SE of 6 mice per group; $P < 0.05$ for overall Kruskal–Wallis test at week 6; cixutumumab was different from the combination therapy. D, growth curve for A2780 xenografts. Results are means ± SE of 5 mice per group, $P < 0.05$ for overall ANOVA test at day 17. Control was different from all other groups and cixutumumab alone was different from bevacizumab and the combination therapy.

Treatment with bevacizumab and with cixutumumab also inhibited cell proliferation, as assayed by Ki67 staining in SKOV3 and A2780 xenografts. The combination cixutumumab and bevacizumab suppressed Ki67, but not to a greater extent than each agent alone (Fig. 5A and B, and Supplementary Fig. S3C, $P < 0.05$ for overall test). Decreased in Akt phosphorylation as measured by immunohistochemistry was induced numerically by both cixutumumab and bevacizumab, but the results were not statistically significant (Fig. 5C and D). These data support that cixutumumab and bevacizumab inhibit tumor growth *in vivo*, by suppressing angiogenesis, cell proliferation, and enhancing apoptosis.

Discussion

Blockade of tumor angiogenesis represents a promising targeted therapy in ovarian cancer, however its effects are transitory and impact on overall survival is not proven (22). Identification of rational combinations to improve the efficacy of antiangiogenic drugs is therefore imperative and represents an unmet need. The goal of this study was to gain a deeper understanding of the adaptive response to anti-VEGF therapy in ovarian cancer models and to identify pathways that are potentially responsible for tumor escape under continued treatment with bevacizumab.

Because one of the proposed resistance mechanisms to anti-VEGF therapy is switch to and reliance on alternative angiogenic pathways, we focused on discovering angiogenesis-related genes altered in tumors exposed to bevacizumab. Interestingly gene expression array analysis did not identify altered expression of the VEGF family factors during bevacizumab treatment and this was confirmed by qRT-PCR for VEGF-A in ovarian xenografts. However, IGF-1 upregulation was detected and was the common denominator in 2 independent xenograft models tested versus the corresponding vehicle-treated controls. Interestingly IGF-1, as measured by gene expression arrays, was not significantly upregulated in SKOV3 xenografts after 4 weeks of bevacizumab treatment (e.g., at the point of maximal tumor response, Fig. 1); but emerged as an upregulated transcript in tumors resistant (A2780) or persistent (SKOV3) during treatment with bevacizumab. The interest in this candidate gene was further increased by the availability of several agents targeting this pathway, currently being evaluated in clinical trials (32) and the significance of the pathway in ovarian cancer. IGF-1 stimulates growth of ovarian xenografts (33) and inhibition of the pathway with a neutralizing anti-IGF-1R antibody blocked tumor growth and reduced receptor signaling through IRS-1, PKC, mitogen-activated protein kinase (MAPK), and phosphoinositide 3-kinase (PI3K)-AKT pathways (33, 34). IGF-1 expression in ovarian tumors is associated with aggressive disease progression and increased angiogenesis through both autocrine and paracrine effects (35). Furthermore, IGF-1 receptor expression levels correlate with cisplatin resistance in ovarian cancer cell lines (34). Collectively, these data support a role of the IGF pathway in progression of ovarian cancer. To our knowledge, our study links for the first time IGF-1 upregulation to escape during AAT.

For the experiments included in this report we used cixutumumab, an antibody against IGF-1 receptor. Cixutumumab downregulated the expression levels of IGF-1 receptor in HUVEC and in SKOV3 cells and downregulated VEGFR-2 in HUVEC cells, acting in a synergistic manner with bevacizumab. The observed synergistic effect of bevacizumab and cixutumumab

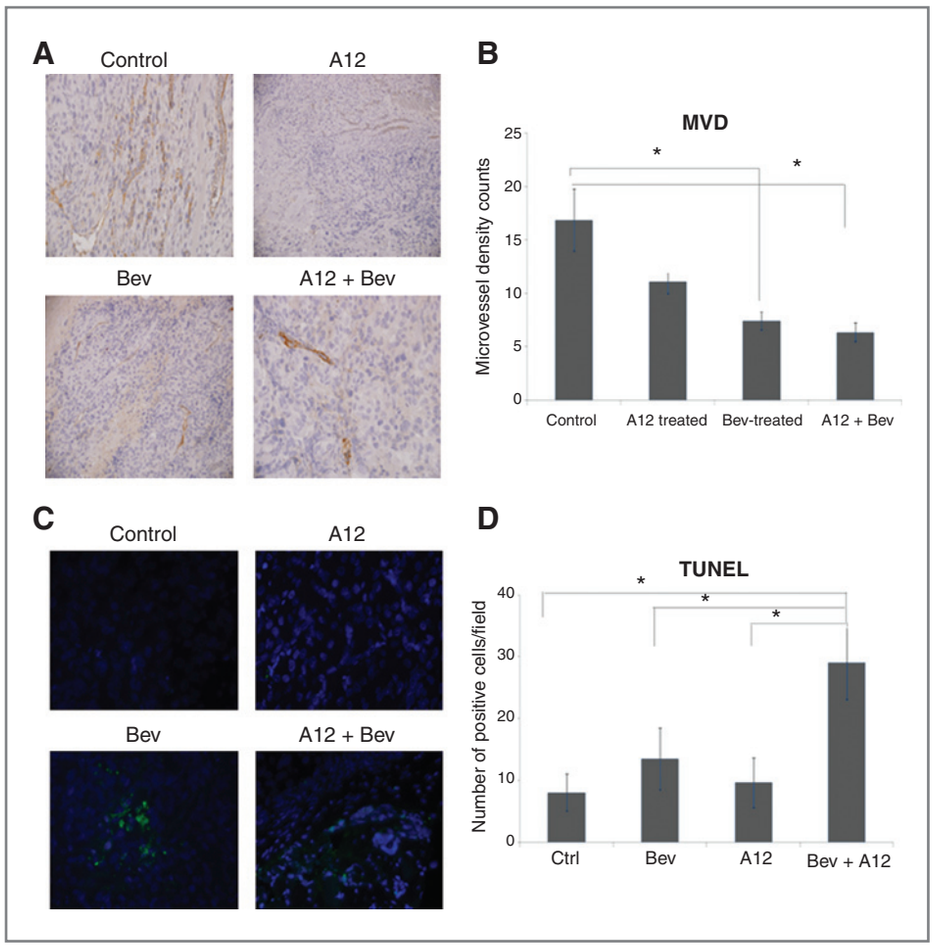

Figure 4. MVD and apoptosis in SKOV3 xenografts treated with control, bevacizumab, cixutumumab, and combination bevacizumab and cixutumumab. A, representative immunohistochemical staining for CD31 shows microvessel density in control, cixutumumab, bevacizumab, and combination-treated xenografts (×100 magnification). B, quantification of microvessel counts was carried out in 5 HPF per specimen in the 4 groups. Results are means of counts in 5 HPF ± SE of 3 specimens per group; results of overall Kruskal–Wallis test were not statistically significant; the 2 bevacizumab groups combined were different from control. C, representative TUNEL immunofluorescent staining in control-, cixutumumab-, bevacizumab-, and combination-treated xenografts. D, quantification of positive cells in the TUNEL assay. Results are means of average counts in 5 HPF per specimen ± SE (3 specimens/group). The overall ANOVA test was significant and combination therapy was significantly different from both single agents and the control.

in vivo supports the hypothesis that IGF-1 induction is part of a key adaptive mechanism for tumor cells, potentially under the selection pressure in the microenvironment of bevacizumab-treated tumors. While our original screen was aimed at the human cellular component of the tumors, and revealed upregulation of human IGF-1, our model affords the investigation of the stromal contribution using species-specific primers. Thus, we confirmed that stroma represents a major source of IGF-1 in the resistant tumors. As cixutumumab cross-reacts with the mouse IGF-1 binding to receptors on the tumor cells, this component is also neutralized by the antibody used, and may contribute to the antitumor effect observed. However, at this point we cannot reliably separate the specific contributions of these 2 compartments to the tumor supporting IGF-1 pool.

The molecular mechanism of IGF-1 induction in our models remains an open question. The complexity of microenvironmental stress potentially relevant for tumor adaptation to bevacizumab (increased hypoxia, nutrient deprivation, more acidic pH) poses a considerable challenge for reconstructing this model *in vitro*. For example, exposure of ovarian cancer cells *in vitro* to hypoxia or to glucose deprivation failed to induce IGF-1 (not shown). Exposure of ovarian cancer cells to both hypoxia and glucose deprivation caused cell death in less than 6 hours. However, the relevance of hypoxia to the mechanism identified here cannot be ruled out simply based on this simplified approach. We have documented hypoxia in ovarian cancer xenografts exposed to bevacizumab by measuring expression levels for 2 known hypoxia-inducible target genes, carbonic anhydrase 9 (CA9), and microRNA-210 (Supplementary Fig. S3). Furthermore, it is documented that conditions in the tumor microenvironment, such as hypoxia, can lead to enhanced responsiveness to IGF-1 (36), which might explain the reliance on this specific pathway as an adaptive mechanism to antiangiogenic treatment.

In addition, a mechanistic clue for IGF-1 induction may be provided by STAT-5b, which we found to be robustly upregulated in bevacizumab-treated tumors. STAT-5b is both a hypoxia-inducible factor (37, 38) and a well-recognized trigger for IGF-1 secretion (29, 39). STAT-5b is an important regulator of cancer cell survival through modulation of antiapoptotic signals via Bcl-xL in prostate and breast cancer and leukemia (40), 41, 42). STAT-5b along with NF-κB complex's Rel-A subunit have also been

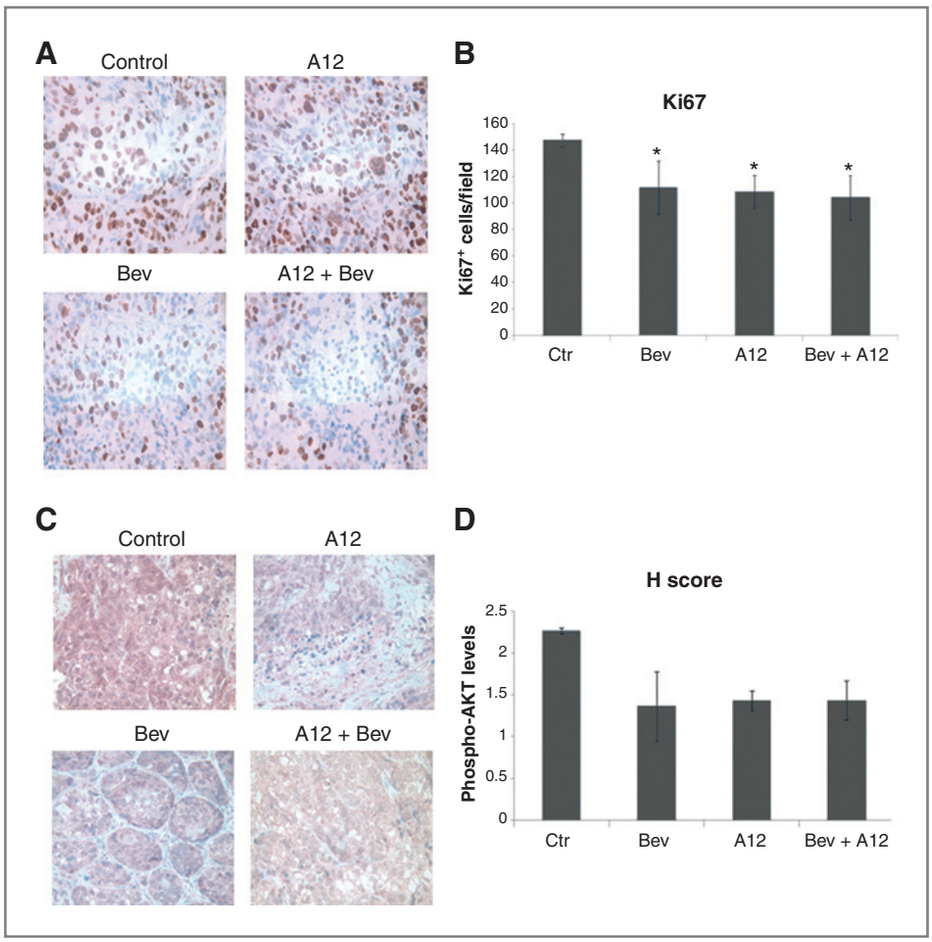

Figure 5. Immunohistochemistry for Ki67 and phospho-Ser^{473}-AKT in control-, cixutumumab-, bevacizumab-, and combination-treated SKOV3 xenografts. A, representative immunohistochemical staining for Ki67 in control-, cixutumumab-, bevacizumab-, and combination-treated xenografts (×100 magnification). B, quantification of Ki67-positive cells was carried out in 5 HPF per specimen in the 4 groups ($n = 3$ specimens per group). The overall ANOVA test was significant and all treatment groups were different from control. Representative C, immunohistochemical staining for phospho-Ser^{473}-AKT in control-, cixutumumab-, bevacizumab-, and combination-treated xenografts (×100 magnification). D, H scores were calculated as described in Materials and Methods. Results are means ± SE of 3 specimens per group; the overall ANOVA test was not statistically significant. The 3 treatment groups combined were different from control.

implicated in carboplatin resistance in ovarian cancer (43), suggesting that this is an important survival pathway in ovarian tumors. In that study, STAT-5b and Rel-A were upregulated in recurrent postchemotherapy ovarian specimens compared with primary tumors, and the simultaneous knockdown of the 2 transcription factors sensitized tumor cells to carboplatin (43). STAT-5b regulates other angiogenic factors and members of the extracellular matrix, such as VEGF-C and collagen type VI and XII (42), and interestingly the JAK-STAT5 signaling axis also regulates ID-1 expression (42, 44). We found ID-1 to be upregulated in bevacizumab-treated xenografts and it is possible that its regulation occurs downstream of STAT signaling under these conditions. Interestingly, at least based on our qRT-PCR data, STAT-5b induction appears more robust in the stromal component of tumors compared with tumor cells, consistent with higher induction of murine IGF-1 in bevacizumab-treated tumors. These observations argue for the importance of the tumor microenvironment in the adaptive response to AAT.

A limitation of our study is the use of subcutaneous, rather than intraperitoneal xenografts. Ovarian tumors usually develop in the peritoneal space that has unique characteristics favoring tumor development. The peritoneum consists of mesothelial cells that cover and protect the viscera. The subperitoneal stroma contains a collagen-based matrix, immune cells, activated fibroblasts, blood vessels, and lymphatics. Several studies have shown an "activated" phenotype associated with ovarian cancer, as opposed to its quiescent state in benign conditions (45). The proinflammatory signature associated with cancer consists of chemokines, cytokines, and growth factors commonly upregulated in the peritoneal milieu (45–47). While tumor cells play a role in the secretion of factors that modulate angiogenesis, more recently it has become accepted that tumor infiltrating cells such as fibroblasts, myeloid cells, immune cells, and endothelial precursors play a crucial role modulating neovascularization (48). Future studies will focus on intraperitoneal xenografts in an effort to better mimic the development of ovarian tumors and metastases in the peritoneal space.

We show that cixutumumab and bevacizumab synergize *in vivo* blocking ovarian tumor growth and angiogenesis. To our knowledge, these data provide the first proof of principle that a combination between anti-VEGF therapy and inactivation of the IGF pathway may provide significant benefit over antiangiogenic drugs as single

agents and support further testing of this or of similar combinations in patients with ovarian cancer.

Disclosure of Potential Conflicts of Interest

No potential conflicts of interest were disclosed.

Acknowledgments

The authors thank Dr. Ruslan Novosyadlyy of ImClone Systems, a wholly-owned subsidiary of Eli Lilly and Company, for providing cixutumumab and comments and Dr. Bakhtior Yakubov for help with manuscript editing.

Grant Support

This work was supported by the American Cancer Society through a Research Scholar Grant and by the U.S. Department of Veterans Affairs through a Merit Award to D. Matei.

The costs of publication of this article were defrayed in part by the payment of page charges. This article must therefore be hereby marked *advertisement* in accordance with 18 U.S.C. Section 1734 solely to indicate this fact.

Received November 28, 2011; revised March 13, 2012; accepted April 5, 2012; published OnlineFirst June 13, 2012.

References

1. Carmeliet P, Jain RK. Angiogenesis in cancer and other diseases. Nature 2000;407:249–57.
2. Ghosh S, Maity P. Isolation and purification of vascular endothelial growth factor (VEGF) from ascitic fluid of ovarian cancer patients. Pathol Oncol Res 2004;10:104–8.
3. Ren J, Xiao YJ, Singh LS, Zhao X, Zhao Z, Feng L, et al. Lysophosphatidic acid is constitutively produced by human peritoneal mesothelial cells and enhances adhesion, migration, and invasion of ovarian cancer cells. Cancer Res 2006;66:3006–14.
4. Matei D, Emerson RE, Lai YC, Baldridge LA, Rao J, Yiannoutsos C, et al. Autocrine activation of PDGFRalpha promotes the progression of ovarian cancer. Oncogene 2006;25:2060–9.
5. Mendiola M, Barriuso J, Redondo A, Marino-Enriquez A, Madero R, Espinosa E, et al. Angiogenesis-related gene expression profile with independent prognostic value in advanced ovarian carcinoma. PLoS ONE 2008;3:e4051.
6. Bamberger ES, Perrett CW. Angiogenesis in epithelian ovarian cancer. Mol Pathol 2002;55:348–59.
7. Shen GH, Kawanami O, Shimizu H, Jin E, Araki T, Sugisaki Y. Prognostic significance of vascular endothelial growht factor expression in human ovarian carcinoma. Br J Cancer 2000;83:196–203.
8. Goodheart MJ, Rose SL, Fruehauf JP, De Young BR, Buller RE. The relationship of molecular marker s of p53 function and angiogenesis to tprogression of stage I epithelial ovarian cancer. Clin Cancer Res 2005;11:3733–42.
9. Hefler LA, Mustea A, Konsgen D, Concin N, Tanner B, Strick R, Heinze G, et al. Vascular endothelial growth factor gene polymorphisims are associated with prognosis in ovarian cancer. Clin Cancer Res 2007;13:898–901.
10. Gadducci A, Ferdeghini M, Fanucchi A, Annicchiarico C, Ciampi B, Prontera C. Serum preoperative vascular endothelial growth factor (VEGF) in epithelial ovarian cancer: relationship with prognostic variables and clinical outcome. Anticancer Res 1999;19:1401–5.
11. Folkman J. A new link in ovarian cancer angiogenesis: lysophosphatidic acid and vascular endothelial growth factor expression. J Natl Cancer Inst 2001;93:734–5.
12. Tempfer C, Obermair A, Hefler L, Haeusler G, Gitsch G, Kainz CVascular endothelial growth factor serum concentrations in ovarian cancer. Obstet Gynecol 1998;92:360–3.
13. Huynh H, Teo CC, Soo KC. Bevacizumab and rapamycin inhibit tumor growth in peritoneal model of human ovarian cancer. Mol Cancer Ther 2007;6;2959–66.
14. Carmeliet P. Angiogenesis in life, disease and medicine. Nature 2005;438:932–6.
15. Risau W. Mechanisms of angiogenesis. Nature 1997;386:671–4.
16. Selvakumaran M, Yao KS, Feldman MD, O'Dwyer PJ. Antitumor effect of the angiogenesis inhibitor bevacizumab is dependent on susceptibility of tumors to hypoxia-induced apoptosis. Biochem Pharmacol 2008;75:627–38.
17. Burger RA. Experience with bevacizumab in the management of epithelial ovarian cancer. J Clin Oncol 2007;25:2902–8.
18. Cannistra SA, Matulonis UA, Penson RT, Hambleton J, Dupont J, Mackey H, et al. Phase II study of bevacizumab in patients with platinum-resistant ovarian cancer or peritoneal serous cancer. J Clin Oncol 2007;25:5180–6.
19. Garcia AA, Hirte H, Fleming G, Yang D, Tsao-Wei DD, Roman L, et al. Phase II clinical trial of bevacizumab and low-dose metronomic oral cyclophosphamide in recurrent ovarian cancer: a trial of the California, Chicago, and Princess Margaret Hospital phase II consortia. J Clin Oncol 2008;26:76–82.
20. Burger RA, Sill MW, Monk BJ, Greer BE, Sorosky JI. Phase II trial of bevacizumab in persistent or recurrent epithelial ovarian cancer or primary peritoneal cancer: a Gynecologic Oncology Group Study. J Clin Oncol 2007;25:5165–71.
21. Burger RA, Brady MF, Bookman MA, Fleming GF, Monk BJ, Huang H, et al. Incorporation of bevacizumab in the primary treatment of ovarian cancer. N Engl J Med 2011;365:2473–83.
22. Perren TJ, Swart AM, Pfisterer J, Ledermann JA, Pujade-Lauraine E, Kristensen G, et al. A phase 3 trial of bevacizumab in ovarian cancer. N Engl J Med 2011;365:2484–96.
23. Paez-Ribes M, Allen E, Hudock J, Takeda T, Okuyama H, Vinals F, et al. Antiangiogenic therapy elicits malignant progression of tumors to increased local invasion and distant metastasis. Cancer Cell 2009;15:220–31.
24. Bergers G, Hanahan D. Modes of resistance to anti-angiogenic therapy. Nat Rev Cancer 2008;8:592–603.
25. Casanovas O, Hicklin DJ, Bergers G, Hanahan D. Drug resistance by evasion of antiangiogenic targeting of VEGF signaling in late-stage pancreatic islet tumors. Cancer Cell 2005;8:299–309.
26. Shojaei F, Wu X, Zhong C, Yu L, Liang XH, Yao J, et al. Bv8 regulates myeloid-cell-dependent tumour angiogenesis. Nature 2007;450:825–31.
27. Shojaei F, Wu X, Malik AK, Zhong C, Baldwin ME, Schanz S, et al. Tumor refractoriness to anti-VEGF treatment is mediated by CD11b+Gr1+ myeloid cells. Nat Biotechnol 2007;25:911–20.
28. Sachdev D, Zhang X, Matise I, Gaillard-Kelly M, Yee D. The type I insulin-like growth factor receptor regulates cancer metastasis independently of primary tumor growth by promoting invasion and survival. Oncogene 2010;29:251–62.
29. Hwa V, Little B, Kofoed EM, Rosenfeld RG. Transcriptional regulation of insulin-like growth factor-I by interferon-gamma requires STAT-5b. J Biol Chem 2004;279:2728–36.
30. Eleswarapu S, Gu Z, Jiang H. Growth hormone regulation of insulin-like growth factor-I gene expression may be mediated by multiple distal signal transducer and activator of transcription 5 binding sites. Endocrinology 2008;149:2230–40.
31. Rowinsky EK, Schwartz JD, Zojwalla N, Youssoufian H, Fox F, Pultar P, et al. Blockade of insulin-like growth factor type-1 receptor with cixutumumab (IMC-A12): a novel approach to treatment for multiple cancers. Curr Drug Targets 2011;12:2016–33.
32. Rowinsky EK, Youssoufian H, Tonra JR, Solomon P, Burtrum D, Ludwig DL. IMC-A12, a human IgG1 monoclonal antibody to the insulin-like growth factor I receptor. Clin Cancer Res 2007;13:5549s–55s.
33. Wang Y, Hailey J, Williams D, Wang Y, Lipari P, Malkowski M, et al. Inhibition of insulin-like growth factor-1 receptor (IGF-1R) signaling and tumor cell growth by a fully human neutralizing anti-IGF-IR antibody. Mol Cancer Ther 2005;4:1214–21.

34. Eckstein N, Servan K, Hildebrandt B, Politz A, von Jonquieres G, Wolf-Kummeth S, et al. Hyperactivation of the insulin-like growth factor receptor I signaling pathway is an essential event for cisplatin resistance of ovarian cancer cells. Cancer Res 2009;69:2996–3003.
35. Cao Z, Liu LZ, Dixon DA, Zheng JZ, Chandran B, Jiang BH. Insulin-like growth factor-I induces cyclooxygenase-2 expression via PI3K, MAPK and PKC signaling pathways in human ovarian cancer cells. Cell Signal 2007;19:1542–53.
36. Clemmons DR. Modifying IGF1 activity: an approach to treat endocrine disorders, atherosclerosis and cancer. Nat Rev Drug Discov 2007;6:821–33.
37. Joung YH, Lee MY, Lim EJ, Kim MS, Hwang TS, Kim SY, et al. Hypoxia activates the IGF-1 expression through STAT5b in human HepG2 cells. Biochem Biophys Res Commun 2007;358:733–8.
38. Joung YH, Lim EJ, Lee MY, Park JH, Ye SK, Park EU, et al. Hypoxia activates the cyclin D1 promoter via the Jak2/STAT5b pathway in breast cancer cells. Exp Mol Med 2005;37:353–64.
39. Fleenor D, Arumugam R, Freemark M. Growth hormone and prolactin receptors in adipogenesis: STAT-5 activation, suppressors of cytokine signaling, and regulation of insulin-like growth factor I. Horm Res 2006;66:101–10.
40. Battle TE, Frank DA. The role of STATs in apoptosis. Curr Mol Med 2002;2:381–92.
41. Caffarel MM, Zaragoza R, Pensa S, Li J, Green AR, Watson CJ. Constitutive activation of JAK2 in mammary epithelium elevates Stat5 signalling, promotes alveologenesis and resistance to cell death, and contributes to tumourigenesis. Cell Death Differ 2012;19:511–22.
42. Gu L, Dagvadorj A, Lutz J, Leiby B, Bonuccelli G, Lisanti MP, et al. Transcription factor Stat3 stimulates metastatic behavior of human prostate cancer cells *in vivo*, whereas Stat5b has a preferential role in the promotion of prostate cancer cell viability and tumor growth. Am J Pathol 2010;176:1959–72.
43. Jinawath N, Vasoontara C, Jinawath A, Fang X, Zhao K, Yap KL, et al. Oncoproteomic analysis reveals co-upregulation of RELA and STAT5 in carboplatin resistant ovarian carcinoma. PLoS One 2010;5:e11198.
44. Wood AD, Chen E, Donaldson IJ, Hattangadi S, Burke KA, Dawson MA, et al. ID1 promotes expansion and survival of primary erythroid cells and is a target of JAK2V617F-STAT5 signaling. Blood 2009;114:1820–30.
45. Freedman RS, Deavers M, Liu J, Wang E. Peritoneal inflammation—a microenvironment for epithelial ovarian cancer (EOC). J Transl Med 2004;2:23.
46. Said N, Socha MJ, Olearczyk JJ, Elmarakby AA, Imig JD, Motamed K. Normalization of the ovarian cancer microenvironment by SPARC. Mol Cancer Res 2007;5:1015–30.
47. Hurteau J, Rodriguez GC, Whitaker RS, Shah S, Mills G, Bast RC, et al. Transforming growth factor-beta inhibits proliferation of human ovarian cancer cells obtained from ascites. Cancer 1994;74:93–9.
48. Nozawa H, Chiu C, Hanahan D. Infiltrating neutrophils mediate the initial angiogenic switch in a mouse model of multistage carcinogenesis. Proc Natl Acad Sci U S A 2006;103:12493–8.